Journal of Engineering Mechanics and Machinery (2023)
Clausius Scientific Press, Canada
DOI: 10.23977/jemm.2023.080101
ISSN 2371-9133 Vol. 8 Num. 1

Wind turbine blades load matching method under biaxial fatigue test

Dewang Li[1,a,*]

[1]Lanzhou University of Technology, Lanzhou, 730000, China
[a]1042880582@qq.com
[*]Corresponding author

Keywords: Biaxial loading, wind turbine blades, fatigue test, load matching

Abstract: In order to improve the fatigue test accuracy and efficiency of full-scale structure of wind turbine blades, an effective load matching method for full-scale structure fatigue test of wind turbine blades under biaxial loading is proposed. The blade biaxial loading fatigue test scheme is designed. The transfer matrix method is used to calculate the test bending moment under biaxial loading. The particle swarm optimization algorithm is designed to optimize the position and mass of the excitation device in the flap-wise and edgewise directions and the position, mass and quantity of the fixed counterweight. Based on this, the calculation model of the test bending moment and the data of the target bending moment are integrated into the particle swarm optimization algorithm to achieve the optimal matching of the biaxial loading fatigue test load, Finally, a numerical example is given to verify it. The results show that this method can make the test load closer to the target load, further accelerate the popularization of biaxial loading fatigue test, and provide a certain theoretical reference and application value for engineering practice.

1. Introduction

Wind turbine blade is an important component of wind power system to obtain wind energy. It is necessary to carry out quality inspection on the blade before it is put into the market through full-scale fatigue test, so as to ensure that the blade can reach the service life of 20 years [1-3]. The key to fatigue testing technology is the test loading system and the test load.

Blade fatigue test loading systems can be classified according to the direction of test loading and the form of loading. According to the test loading direction, the full-size structure fatigue test is mainly divided into uniaxial loading and biaxial loading. Single axis loading is tested in one direction. Biaxial fatigue test is to conduct the flap-wise and edgewise direction at the same time for performance testing, compared with single-axis loading way, the advantages of biaxial loading way is more obvious. First, the way of biaxial loading usually will load simultaneously added to the flap-wise and edgewise direction, more realistic and effective simulation of blade loading situation, improve the test accuracy. Second, simultaneously carry out the flap-wise and edgewise direction loading test, shorten the test cycle time [4-5]. According to the test loading form, the fatigue test of full-scale structures is mainly divided into forced displacement type and resonance excitation type [6]. Compared to the forced displacement type, the resonant excitation type fatigue test system can obtain a large blade amplitude with a small excitation force, and has the advantages of low cost, short test cycle and suitable for large wind turbine blades [7]. Thus, the resonant excitation fatigue test has become the main loading method.

The finite element method and the transfer matrix method are often used in engineering to calculate test loads. The finite element method is the main tool for wind turbine blade design and analysis, but the modelling process is cumbersome and the efficiency of the calculation cannot be guaranteed. The transfer matrix method is widely used in load calculations due to its high computational efficiency, clear physical meaning and ease of model construction. Greaves used a genetic algorithm to optimize the distribution of loads for resonantly excited biaxially loaded fatigue test, but this algorithm suffers from low search efficiency and a more complex programming process. In addition, the genetic algorithm cannot solve the problem of deterministic termination conditions and its own slow convergence speed, so it is not applicable. Zhang and Lu et al used a particle swarm algorithm for load matching, which is less difficult compared with the above algorithm.

Therefore, this paper proposes a biaxial loaded wind turbine blade fatigue test load matching method that integrates the transfer matrix method into a particle swarm optimization algorithm from the perspective of dynamics analysis and engineering optimization, in order to test the blade's ability to withstand the target load, and validates the proposed method with an MW-scale blade.

2. Fatigue test scheme design for biaxial loading

Considering that the inherent frequencies in the flap-wise and edgewise direction are not equal, two excitation devices should be installed along the blade spreading direction for biaxial loading fatigue test. Therefore, assume that the edgewise direction of the excitation device is placed in the d section, the total mass is ΔM^{e}, the fixed mass is m^{e}, the rotating mass is Δm^{e}, flap-wise direction of the excitation device is placed in the k section, the total mass is ΔM^{f}, the fixed mass is m^{f}, the rotating mass is Δm^{f}, where the upper corner f , e represent the flap-wise direction and edgewise direction respectively. Then the schematic diagram of the biaxial loading fatigue test scheme is shown in Figure 1.

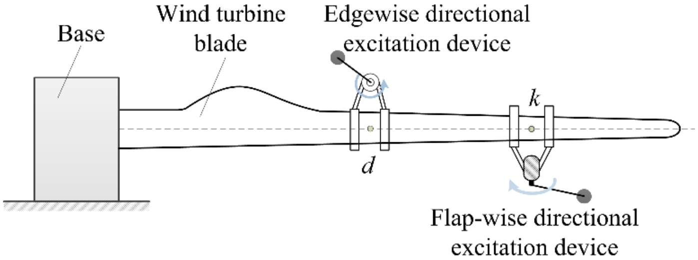

Figure 1: Schematic diagram of full-scale fatigue test of blade with biaxial loading

3. Fatigue test load calculation method for biaxial loading

Assuming that the vibration in the flap-wise and edgewise directions are independent, based on the blade equivalent cantilever beam model, the state quantities of each section of the blade are calculated by the transfer matrix method from the flap-wise and edgewise directions respectively, and finally the test bending moment of the whole blade in both directions is derived. Based on the biaxial loading fatigue test scheme, then the test bending moment calculation process of the biaxial loading fatigue test is divided into five steps.

(1) Discrete modelling of the blade under biaxial loading

From engineering mechanics, it is known that the blade with fixed root tip activity can be equated to a cantilever beam model, which can be discretized into a finite number of n sections along the spreading direction according to the section properties, and marked by the blade root towards the blade tip with increasing serial number, and the two adjacent sections and the middle mass-free elastic beam together form a unit. According to the position of the excitation device in the flap-wise and edgewise directions, the discrete model of the blade under biaxial loading is established, as shown in Figure 2.

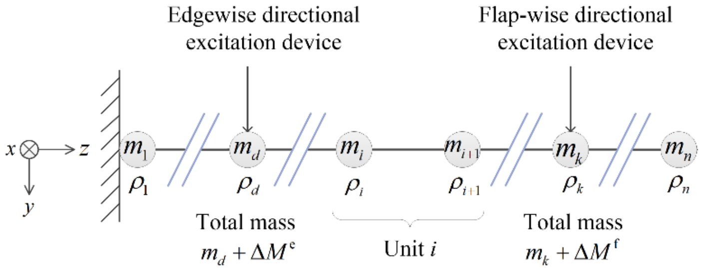

Figure 2: Discrete model of blade under biaxial loading

(2) Establish the transfer equations in the direction of the flap-wise and the direction of the edgewise

Since the blade is a continuously varying elastic member, the bending stiffness EI_i of section i and the bending stiffness EI_{i+1} of section i+1 can be averaged and then assigned to the elastic beam segment i. The bending stiffness of the elastic beam segment in the flap-wise and edgewise directions can be approximated as:

$$\begin{cases} \overline{EI_i^{\mathrm{f}}} = \dfrac{EI_i^{\mathrm{f}} + EI_{i+1}^{\mathrm{f}}}{2} \\ \overline{EI_i^{\mathrm{e}}} = \dfrac{EI_i^{\mathrm{e}} + EI_{i+1}^{\mathrm{e}}}{2} \end{cases} \tag{1}$$

The state quantities for each section in both directions can be obtained from the section properties as

$$\begin{cases} \boldsymbol{S}_i^{\mathrm{f}} = \begin{bmatrix} y_i^{\mathrm{f}} & \theta_i^{\mathrm{f}} & M_i^{\mathrm{f}} & Q_i^{\mathrm{f}} \end{bmatrix}^T \\ \boldsymbol{S}_i^{\mathrm{e}} = \begin{bmatrix} y_i^{\mathrm{e}} & \theta_i^{\mathrm{e}} & M_i^{\mathrm{e}} & Q_i^{\mathrm{e}} \end{bmatrix}^T \end{cases} \tag{2}$$

Where, y_i, θ_i, M_i, Q_i are the deflection, angle of rotation, bending moment and shear force of the i-th section respectively. Since the total masses of the excitation devices in the flap-wise and edgewise directions are ΔM^{f} and ΔM^{e} respectively, the total masses m_k^* and m_d^* of sections k and d after the arrangement of the excitation devices are

$$\begin{cases} m_k^* = m_k + \Delta M^{\mathrm{f}} \\ m_d^* = m_d + \Delta M^{\mathrm{e}} \end{cases} \tag{3}$$

The flap-wise direction excitation force F^{f} is applied on section k, and the edgewise direction excitation force F^{e} is applied on section d. Then the excitation forces F^{f} and F^{e} are:

$$\begin{cases} F^{\mathrm{f}} = \Delta m^{\mathrm{f}} (\omega^{\mathrm{f}})^2 A^{\mathrm{f}} \\ F^{\mathrm{e}} = \Delta m^{\mathrm{e}} (\omega^{\mathrm{e}})^2 A^{\mathrm{e}} \end{cases} \tag{4}$$

where ω is the intrinsic circular frequency, unit rad/s, A is the radius of motion of the rotating mass, unit m.

The dynamics of the blade edgewise direction, d-1 units of the force situation as shown in Figure 3, then establish the state quantity transfer relationship between the right end of the section and the left end of the section.

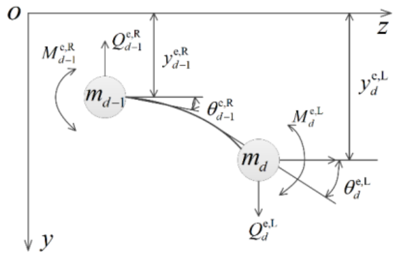

Figure 3: Diagram of the forces between sections of unit d-1

The excitation force F^{e} in the direction of edgewise acts on the section d, and the force is shown in Figure 4. Then the shear force Q_d^{e} transfer relationship between the left and right sides of the excitation point d is shown in (5).

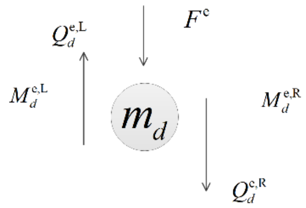

Figure 4: Section d force diagram

$$Q_d^{e,R} = Q_d^{e,R} + (\omega^{e})^2 m_d^{*} y_d^{e} - F^{e} \tag{5}$$

Thus, the transfer relation between the state quantities at the right and left ends of section d can be deduced as follows:

$$\begin{bmatrix} y_d^{e} \\ \theta_d^{e} \\ M_d^{e} \\ Q_d^{e} \end{bmatrix}^{R} = \begin{bmatrix} 1 & 0 & 0 & 0 \\ 0 & 1 & 0 & 0 \\ 0 & 0 & 1 & 0 \\ m_d^{*}(\omega^{e})^2 & 0 & 0 & 1 \end{bmatrix} \begin{bmatrix} y_d^{e} \\ \theta_d^{e} \\ M_d^{e} \\ Q_d^{e} \end{bmatrix}^{L} - \begin{bmatrix} 0 \\ 0 \\ 0 \\ 1 \end{bmatrix} F^{e} \tag{6}$$

The transfer equation from $\boldsymbol{S}_{d-1}^{e}$ to $\boldsymbol{S}_d^{e}$ can be further obtained as:

$$\begin{bmatrix} y_d^{e} \\ \theta_d^{e} \\ M_d^{e} \\ Q_d^{e} \end{bmatrix}^{R} = \begin{bmatrix} 1 & l_{d-1} & \dfrac{l_{d-1}^2}{2EI_{d-1}^{e}} & \dfrac{l_{d-1}^3}{6EI_{d-1}^{e}} \\ 0 & 1 & \dfrac{l_{d-1}}{EI_{d-1}^{e}} & \dfrac{l_{d-1}^2}{2EI_{d-1}^{e}} \\ 0 & 0 & 1 & l_{d-1} \\ m_d^{*}(\omega^{e})^2 & m_d^{*}(\omega^{e})^2 l_i & \dfrac{m_d^{*}(\omega^{e})^2 l_{d-1}^2}{2EI_{d-1}^{e}} & (1+\dfrac{m_d^{*}(\omega^{e})^2 l_{d-1}^3}{6EI_{d-1}^{e}}) \end{bmatrix} \begin{bmatrix} y_{d-1}^{e} \\ \theta_{d-1}^{e} \\ M_{d-1}^{e} \\ Q_{d-1}^{e} \end{bmatrix}^{R} - \begin{bmatrix} 0 \\ 0 \\ 0 \\ 1 \end{bmatrix} F^{e} \tag{7}$$

For the analysis of the blade edgewise direction, the flap-wise direction excitation device is equivalent to a fixed counterweight added to the section k. According to the transfer matrix $\boldsymbol{T}_{k-1}^{e}$ from $\boldsymbol{S}_{k-1}^{e}$ to $\boldsymbol{S}_k^{e}$, the total transfer of the edgewise direction from the state quantity $\boldsymbol{S}_n^{e}$ at the tip of the blade section to the state quantity $\boldsymbol{S}_1^{e}$ at the root of the blade section is given by:

$$\boldsymbol{S}_n^{\mathrm{e}} = \boldsymbol{T}_{n-1}^{\mathrm{e}} \cdots \boldsymbol{T}_k^{\mathrm{e}} \cdots \boldsymbol{T}_d^{\mathrm{e}} (\boldsymbol{T}_{d-1}^{\mathrm{e}} \cdots \boldsymbol{T}_1^{\mathrm{e}} \boldsymbol{S}_1^{\mathrm{e}} - F^{\mathrm{e}}) \tag{8}$$

The flap-wise direction transfer equation is derived in the same way as the edgewise direction transfer equation. It should be noted that the flap-wise directional excitation force F^{f} acts on section k, while the edgewise directional excitation device is equivalent to a fixed counterweight added to section d. The total transfer relationship between the flap-wise directional state quantity $\boldsymbol{S}_n^{\mathrm{f}}$ from the tip section and the root section state quantity $\boldsymbol{S}_1^{\mathrm{f}}$ is:

$$\boldsymbol{S}_n^{\mathrm{f}} = \boldsymbol{T}_{n-1}^{\mathrm{f}} \cdots \boldsymbol{T}_k^{\mathrm{f}} (\boldsymbol{T}_{k-1}^{\mathrm{f}} \cdots \boldsymbol{T}_d^{\mathrm{f}} \cdots \boldsymbol{T}_1^{\mathrm{f}} \boldsymbol{S}_1^{\mathrm{f}} - F^{\mathrm{f}}) \tag{9}$$

For a root-fixed blade, the boundary conditions are as follows:

$$\begin{cases} y_1^{\mathrm{R}} = 0 \\ \theta_1^{\mathrm{R}} = 0 \\ M_1^{\mathrm{R}} = \max \\ Q_1^{\mathrm{R}} = \max \end{cases} \begin{cases} y_n^{\mathrm{R}} = \max \\ \theta_n^{\mathrm{R}} = \max \\ M_n^{\mathrm{R}} = 0 \\ Q_n^{\mathrm{R}} = 0 \end{cases} \tag{10}$$

Therefore, by bringing the tip and root constraints into the total transfer relationship in the flap-wise and edgewise directions respectively, the transfer equations in both directions are obtained.

(3) Solve for the inherent frequencies in the flap-wise and edgewise direction

The characteristic equations of the fatigue test system in the flap-wise and edgewise directions can be obtained from the transfer equations, which are functions of the inherent frequencies. According to the idea of engineering optimization, the inherent frequencies in the flap-wise and edgewise directions are solved using a single-objective particle swarm optimization algorithm to obtain the inherent frequencies ω^{f} and ω^{e}.

(4) Calculate the test bending moment for each section in the flap-wise direction and the edgewise direction.

The inherent frequencies of the flap-wise and edgewise directions are substituted into the respective total transfer equations the test bending moment distribution of the whole blade under the biaxial loading fatigue test condition can be obtained.

4. Fatigue test load distribution optimization method for biaxial loading

Considering that the test load under the blade fatigue test conditions is determined by the blade self-weight, counterweight mass and other factors, these parameters determine whether the test bending moment is consistent with the target bending moment. Therefore, from the perspective of engineering optimization, this paper uses the particle swarm optimization algorithm to find the optimum of the above parameters and to optimize the distribution of the test load in the critical area of the blade by controlling the error value between the test bending moment and the target bending moment within the specified range, so as to determine the loading scheme of the blade fatigue test with biaxial loading.

4.1. Conversion from bi-objective to single-objective optimisation

4.1.1. Bi-objective optimization model

This loading scheme is illustrated with a flap-wise direction excitation device, a edgewise direction excitation device and a fixed counterweight.

The optimization variables are:

$$X = \left[x^{\mathrm{f}}, x^{\mathrm{e}}, x, \Delta m^{\mathrm{f}}, \Delta m^{\mathrm{e}}, \Delta m \right]^{\mathrm{T}} \tag{11}$$

Where, x^{f}, x^{e}, x are the position of the flap-wise direction excitation device, the position of the edgewise direction excitation device and the position of the fixed counterweight, unit m, Δm is the fixed counterweight mass, unit kg.

The objective function is:

$$\begin{cases} \min(M_{i,\mathrm{test}}^{\mathrm{f}} - M_{i,\mathrm{target}}^{\mathrm{f}}) \\ \min(M_{i,\mathrm{test}}^{\mathrm{e}} - M_{i,\mathrm{target}}^{\mathrm{e}}) \end{cases} \tag{12}$$

where $M_{\mathrm{test}}^{\mathrm{f}}$ is the test moment in the flap-wise direction, $M_{\mathrm{target}}^{\mathrm{f}}$ is the target moment in the flap-wise direction, $M_{\mathrm{test}}^{\mathrm{e}}$ is the test moment in the edgewise direction and $M_{\mathrm{target}}^{\mathrm{e}}$ is the target moment in the edgewise direction.

The boundary conditions for the optimization variables and the objective function are:

$$\begin{cases} 0 < x^{\mathrm{f}} \le L \\ 0 < x^{\mathrm{e}} \le L \\ 0 \le x \le L \\ 0 < \Delta m^{\mathrm{f}} \le m_{\mathrm{m}} \\ 0 < \Delta m^{\mathrm{e}} \le m_{\mathrm{m}} \\ 0 \le \Delta m \le m_{\mathrm{m}}^{*} \end{cases} \quad \begin{cases} M_{i,\mathrm{test}}^{\mathrm{f}} \ge M_{i,\mathrm{target}}^{\mathrm{f}} \\ M_{i,\mathrm{test}}^{\mathrm{e}} \ge M_{i,\mathrm{target}}^{\mathrm{e}} \\ \dfrac{\left| M_{i,\mathrm{test}}^{\mathrm{f}} - M_{i,\mathrm{target}}^{\mathrm{f}} \right|}{M_{i,\mathrm{target}}^{\mathrm{f}}} \le \delta \\ \dfrac{\left| M_{i,\mathrm{test}}^{\mathrm{e}} - M_{i,\mathrm{target}}^{\mathrm{e}} \right|}{M_{i,\mathrm{target}}^{\mathrm{e}}} \le \delta \end{cases} \tag{13}$$

where L is the area of the excitation device and counterweight arrangement, unit m, m_{m} is the upper limit of the rotating mass of the excitation device, unit kg, m_{m}^{*} is the upper limit of the fixed counterweight mass, unit kg, δ is the relative error of the bending moment, which is generally controlled to be no more than 15% to avoid blade failure.

Therefore, the dual-objective function can be transformed into a single-objective function through some connection, and then the single-objective optimization problem can be solved to achieve the solution of the original dual-objective optimization problem.

4.1.2. Conversion of bi-objective optimization to single-objective optimization

There are two points that need to be noted and illustrated when transforming a dual-objective optimization problem to a single-objective optimization problem. First, the different objective functions that perform the transformation need to be independent of each other and have the same properties; second, for the transformation method, which usually uses weight coefficients, the different objective functions must be reasonable in terms of the assignment of weights.

The two objective functions in this paper are the minimum values of the bending moment errors in the flap-wise and edgewise directions respectively, which are independent of each other and have the same nature. Therefore, the transformation relation from dual objective to single objective can be:

$$\begin{gathered} \begin{cases} \min(M_{i,\mathrm{test}}^{\mathrm{f}} - M_{i,\mathrm{target}}^{\mathrm{f}}) \\ \min(M_{i,\mathrm{test}}^{\mathrm{e}} - M_{i,\mathrm{target}}^{\mathrm{e}}) \end{cases} \\ \downarrow \\ \min\left[\alpha(M_{i,\mathrm{test}}^{\mathrm{f}} - M_{i,\mathrm{target}}^{\mathrm{f}}) + \beta(M_{i,\mathrm{test}}^{\mathrm{e}} - M_{i,\mathrm{target}}^{\mathrm{e}}) \right] \end{gathered} \tag{14}$$

where α, β are the weight coefficients of the flap-wise and edgewise direction objective functions, respectively.

Both objective functions are to solve for the minimum bending moment error, with different directions but equally important, and their weight coefficients can be equally distributed, so α and β are both taken to be 0.5. Therefore, the final single objective function is:

$$\min\left[0.5(M^{\mathrm{f}}_{i,\mathrm{test}}-M^{\mathrm{f}}_{i,\mathrm{target}})+0.5(M^{\mathrm{e}}_{i,\mathrm{test}}-M^{\mathrm{e}}_{i,\mathrm{target}})\right] \tag{15}$$

4.2. Optimal modelling of test load distribution

(1) Import of blade fatigue test target bending moment data

The target bending moment data in the direction of the measured blade flap-wise and edgewise directions are imported for facilitate subsequent comparison with the calculated test bending moments.

(2) Import blade related parameters

The data of blade length, mass distribution and bending stiffness distribution in flap-wise and edgewise directions are imported, and the position of each section is clarified according to the discrete model of the blade under biaxial loading condition.

(3) Initialize the position and velocity of each particle of the particle swarm

Given a population size H, the initial position $P_{h,1}$ of the hth particle (h=1,2…H) in the population space is:

$$P_{h,1}=(x^{\mathrm{f}}(1),x^{\mathrm{e}}(1),x(1),\Delta m^{\mathrm{f}}(1),\Delta m^{\mathrm{e}}(1),\Delta m(1)) \tag{16}$$

where $x^{\mathrm{f}}(1)$, $x^{\mathrm{e}}(1)$, $x(1)$, $\Delta m^{\mathrm{f}}(1)$, $\Delta m^{\mathrm{e}}(1)$ and $\Delta m(1)$ are the initial values of the hth particle, which are determined using uniformly distributed random number generation in the given interval.

The initial velocity $V_{h,1}$ of the hth particle in the population space is:

$$V_{h,1}=\varepsilon\cdot P_{h,1} \tag{17}$$

where ε is a normal distribution random number, its mean value is 1, and the standard deviation is 0.1.

(4) Establish the transfer equation and calculate the test bending moment amplitude

After initializing the parameters, the mass of the cross-section of flap-wise and edgewise directional excitation devices and fixed counterweight arrangement is updated to obtain the latest mass distribution data for the blade. Then, according to the process of test load solution, the transmission relations in the flap-wise and edgewise directions are established respectively, and the test moment amplitudes in both directions are calculated.

(5) Define the fitness function

According to the objective function (17) the fitness function d is defined as:

$$\begin{aligned} obj=0.5&\left|\frac{M^{\mathrm{f}}_{i,\mathrm{test}}-M^{\mathrm{f}}_{i,\mathrm{target}}}{M^{\mathrm{f}}_{i,\mathrm{target}}}\right|(M^{\mathrm{f}}_{i,\mathrm{test}}-M^{\mathrm{f}}_{i,\mathrm{target}})^2\\ +0.5&\left|\frac{M^{\mathrm{e}}_{i,\mathrm{test}}-M^{\mathrm{e}}_{i,\mathrm{target}}}{M^{\mathrm{e}}_{i,\mathrm{target}}}\right|(M^{\mathrm{e}}_{i,\mathrm{test}}-M^{\mathrm{e}}_{i,\mathrm{target}})^2 \end{aligned} \tag{18}$$

This fitness function represents the minimum error between the test bending moment and the target bending moment after determining the test loading scheme.

(6) Update individual extremes and population extremes

Define the initial value of the individual extremum $\boldsymbol{Pb}$ to be $P_{h,1}$. As the iterations proceed, $P_{h,1}$ is brought into the fitness function in turn and its value is compared with the fitness value of $\boldsymbol{Pb}_{h,g}$. If the result of $P_{h,g}$ is less than $\boldsymbol{Pb}_{h,g}$, then $P_{h,g}$ replaces $\boldsymbol{Pb}_{h,g}$. The particle with the lowest fitness value in $P_{h,1}$ is used as the initial value for the population extremum Pg. At each iteration, if one of the fitness values of $\boldsymbol{Pb}$ is less than Pg, then its particle replaces Pg.

(7) Update the velocity and position of each particle

The expressions for each particle velocity and position update are as follows:

$$\begin{aligned} V_{h,g+1} = \mu V_{h,g} + c_1 \cdot r_1 \cdot (\boldsymbol{Pb}_{h,g} - P_{h,g}) \\ + c_2 \cdot r_2 \cdot (Pg^{(j)} - P_{h,g}) \end{aligned} \tag{19}$$

$$P_{h,g+1} = P_{h,g} + V_{h,g+1} \tag{20}$$

where G is the total number of iterations (g=1,2…G), μ is the inertia weight, c_1 and c_2 are the learning factors, r_1 and r_2 are randomly distributed in the interval (0,1).

(8) Iterate to find the best and output the optimal result

When the error between the test bending moment and the target bending moment meets the minimum or the iteration reaches the maximum, the calculation ends and the particle position corresponding to a is output; otherwise, it returns to step 4 and iterates again until the optimal result is obtained.

4.3. Analysis of the algorithm

4.3.1. Algorithm blade data and the value of each parameter

This paper takes 68.6m blade related parameters and fatigue test data as an example, the blade is known to be 61.5m long after cutting the blade tip, divided into 34 units, the measured first-order intrinsic frequency in flap-wise and edgewise direction is 0.583Hz and 0.911Hz respectively. The mass distribution of each section of the blade is shown in Figure 5, the bending stiffness distribution of each section in flap-wise and edgewise direction is shown in Figure 6, the target bending moment distribution data of blade flap-wise and edgewise direction are shown in Figure 7.

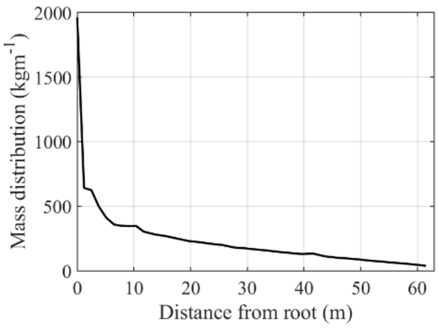

Figure 5: 68.6m wind turbine blade mass distribution

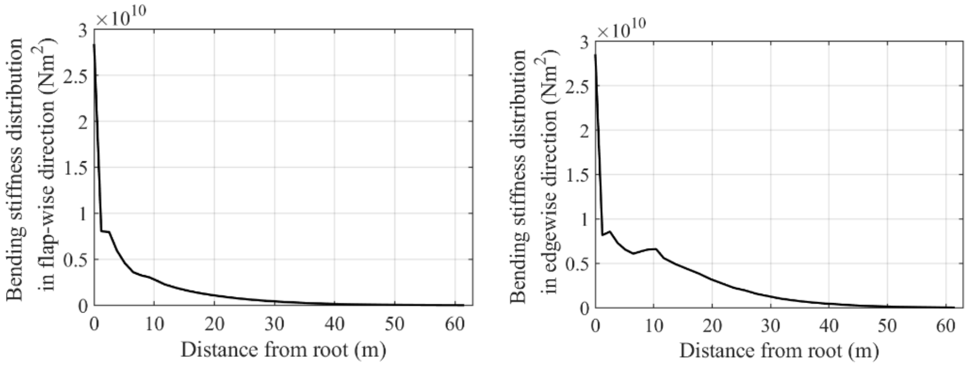

Figure 6: 68.6m wind turbine blade bending stiffness distribution

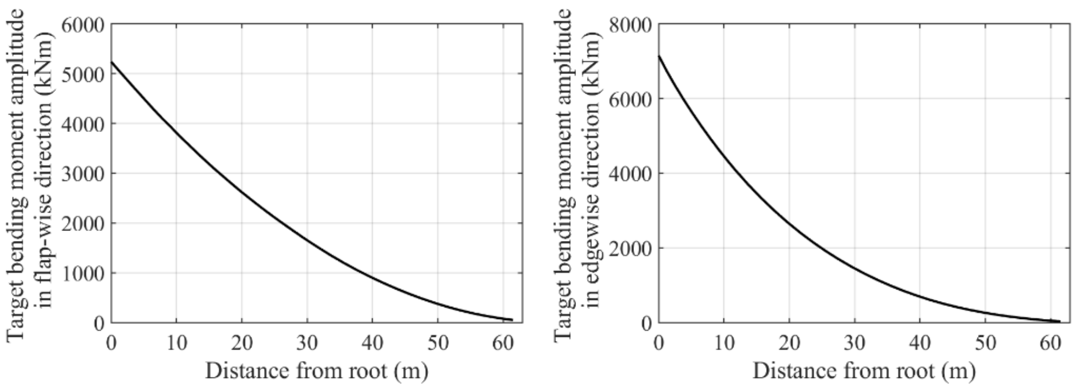

Figure 7: 68.6m wind turbine blade target bending moment distribution

In order to ensure that the test bending moment within a certain section of the blade can meet the fatigue test requirements, according to the biaxial loading fatigue test load distribution optimization method, the relative error of the control bending moment δ does not exceed 10%, this paper will be verified from the blade spreading to 0-70% region.

The optimization parameters are: position x^{f} and rotating mass Δm^{f} of the flap-wise direction excitation device, position x^{e} and rotating mass Δm^{e} of the edgewise direction excitation device, position x and mass Δm of the fixed counterweight. Given that the number of fixed counterweights w also needs to be taken into account in the optimization process, the optimization variables can be expressed as:

$$X^* = \begin{bmatrix} x^{\mathrm{f}}, x^{\mathrm{e}}, \Delta x_1, \Delta x_2, \cdots, \Delta x_w, \\ \Delta m^{\mathrm{f}}, \Delta m^{\mathrm{e}}, \Delta m_1, \Delta m_2, \cdots, \Delta m_w \end{bmatrix}^{\mathrm{T}} \tag{21}$$

where Δx_w is the fixed counterweight position, unit m, Δm_w is the fixed counterweight mass, unit kg, w is the number of fixed counterweights, $w = 1, 2, \cdots, n$. Considering the blade cross-section to apply a larger mass of counterweight will damage the blade, so a single point of the counterweight should not be too large, set its upper limit for 5000kg. In view of the flap-wise direction frequency is less than the frequency of the edgewise direction, then the flap-wise direction to choose a fixed mass of 1500kg of 30kW motor, edgewise direction to choose a fixed mass of 3500kg of 90kW motor, the rotation diameter are 1m, then the rotating mass of the upper limit for 1000kg. The weight distribution area is 30%-80% of the blade spread, so the range of L is about 18m-50m. In summary, the value range of each optimization parameter is shown in Table 1. The parameters in the optimization algorithm are: $G = 200$, $H = 50$, $c_1 = 2$, $c_2 = 2$, $\mu = 0.6$.

Table 1: Range of values for optimization parameters

Parameters	Counterweight area (L/m)	Rotating mass (m_m/kg)	Fixed counterweight mass (m^*/kg)	Bending moment error (δ/%)
Value range	$[18,50]$	$(0,1000]$	$[0,5000]$	$[0,10]$

4.3.2. Example analysis

Blade spread 0-70% of the test area

The optimized loading scheme for the 0-70% test area of the blade spreading direction is shown in Table 2, and the test bending moments and bending moment errors in the flap-wise and edgewise directions, respectively, are shown in Figure 8 and Figure 9. Among them, the optimized vibration frequencies of blade flap-wise and edgewise directions are reduced to 0.557Hz and 0.879Hz respectively, and the frequency errors are 4.5% and 3.51% respectively.

Table 2: Optimized loading scheme for 0-70% test area

Optimization parameters	**Position (m)**	**Total mass (kg)**	**Mass of movement (kg)**
Edgewise direction excitation device	26.9	4019	519
Flap-wise direction excitation device	45.7	2022	522
Fixed counterweight 1	21.4	1810	-
Fixed counterweight 2	42	535	-

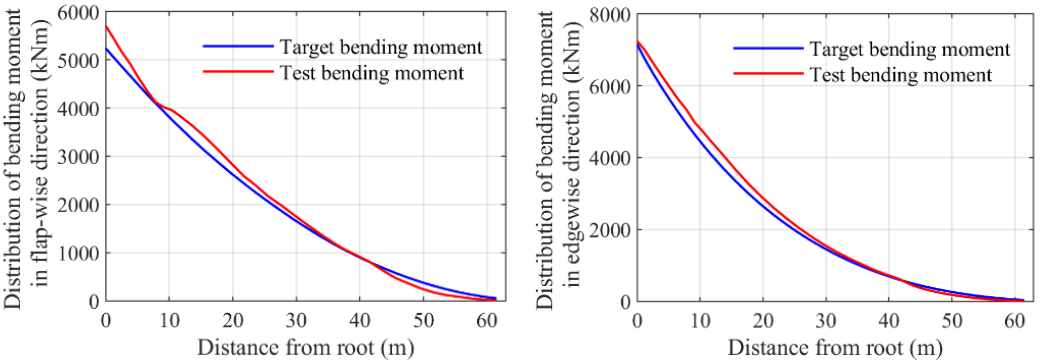

Figure 8: Distribution of target bending moment and test bending moment in the 0-70% test area

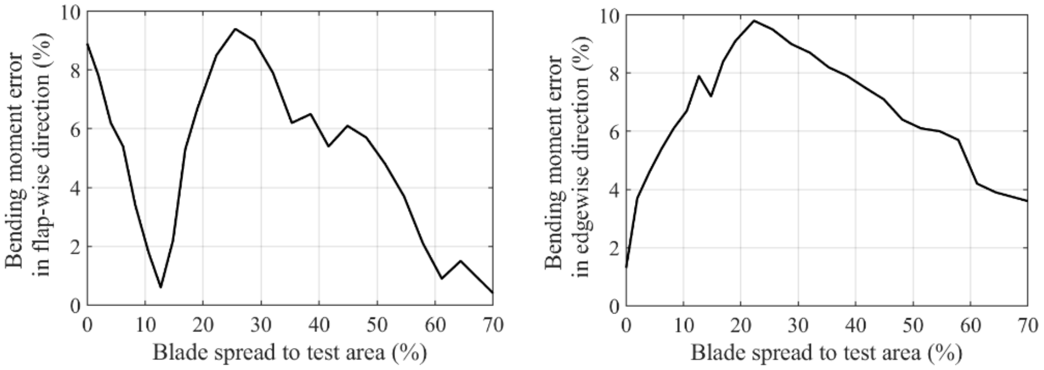

Figure 9: Distribution of bending moment erroring the 0-70% test area

Blade spreading direction 0-70% region of the loading scheme can make the test bending moment is greater than equal to the target bending moment, bending moment error are controlled within 10%, and the frequency error are within 5%, which indicates that the dual-axis loading blade fatigue test load distribution optimization method proposed in this chapter is effective.

5. Conclusion

In this paper, the overall scheme of the biaxially loaded fatigue test is designed under the assumption that the blade flap-wise and edgewise directions are independent of each other, whereby the calculation model of the biaxially loaded test load is established in combination with the transfer matrix method, and the placement position and rotating mass of the excitation device in the flap-wise and edgewise directions as well as the placement position, mass and arrangement number of the fixed counterweight are optimized by using the particle swarm algorithm. The calculation model of the test load is invoked to achieve the load matching of the blade biaxial loading fatigue test. The results of the study show that: through the analysis of the calculation cases, it is found that the frequency error is below 5% and the bending moment error is controlled within 10% in the one test areas of 0-70% of the blade spreading, which meet the test accuracy requirements. The method in this paper not only enables optimize the parameters quickly and accurately, but also provides an effective reference for the blade biaxial loading fatigue test scheme.

References

[1] X. F. Chen, Y. J. Guo, C. B. Xu and H. B. Shang. Review of fault diagnosis and health monitoring for wind power equipment. China Mechanical Engineering, 2020, 31: 175–189.

[2] IEC 61400-23, Wind turbines-part 23: Full-scale structural testing of rotor blades, Switerland: International. Electrotechnical Commission, 2014.

[3] G. H. Liao and J. Z. Wu. Vibration characteristics of bidirectional electric reciprocating loading system of wind turbine blade. Acta Energiae Solaris Sinica, 2021, 42: 380–385.

[4] O. Castroa, P. Berring, K. Branner, C. F. Hvejsel, S. C. Yeniceli and F. Belloni. Bending-moment-based approach to match damage-equivalent strains in fatigue testing. Engineering Structures, 2021, 226: 111325.

[5] C. L. Li, J. F. Zhang, D. G. Zhang and Z. Y. Li. Accuracy research on full-scale test of large wind turbine blade. Composites Science and Engineering, 2021, 4: 83–88+101.

[6] Q. Ma, Z. W. An, J. Q. Gao, H. X. Kou and X. Z. Bai. A method of determining test load for full-scale wind turbine blade fatigue tests. Journal of Mechanical Science and Technology, 2018. 32: 5097–5104.

[7] X. M. Huang, L. A. Zhang, G. M. Yuan and N. Wang. Accuracy improvement on fatigue test of megawatt wind turbine blades by adaptive fuzzy control. Journal of Vibroengineering, 2014, 16: 2631–2638.